

The Nearest Neighbor Alignment of Cluster X-ray Isophotes

Scott W. Chambers^{1,3}, Adrian L. Melott^{1,4} and Christopher J. Miller^{2,5}

ABSTRACT

We examine the orientations of rich galaxy cluster X-ray isophotes with respect to their rich nearest neighbors, using previously determined samples of Abell cluster position angles measured from *Einstein* and *ROSAT* observations. We study subsets of these samples using updated and improved positions and redshifts for Abell/ACO clusters. We find high confidence for alignment, which increases as nearest neighbor distance is restricted. We conclude that there is a strong alignment signal in all this data, consistent with gravitational instability acting on Gaussian perturbations.

Subject headings: clusters of galaxies - Xrays: general — large-scale structure of universe

1. Introduction

A conventional picture suggests that clusters form by hierarchical clustering in which material (gas, galaxies etc.) falls into the cluster along the large-scale interconnecting filamentary structure (Shandarin & Klypin 1984). As a result, clusters, in both optical and X-ray, appear aligned with their neighbors, especially when they are members of the same supercluster. Observationally, this picture has been supported by previous alignment studies (see below), and dynamical evidence of relic drainage along supercluster filaments (Novikov *et al.* 1999).

Most numerical simulations of structure formation by gravitational instability acting on Gaussian initial perturbations predict nearest neighbor alignment on some scale (e.g.

¹Dept. of Physics & Astronomy, Univ. of Kansas, Lawrence, KS 66045

²Dept. of Physics & Astronomy, Carnegie Mellon Univ., Pittsburgh, PA 15213

³willc@kusmos.phsx.ukans.edu

⁴melott@kusmos.phsx.ukans.edu

⁵chrism@fire.phys.cmu.edu

Splinter et al. 1997; Onuora & Thomas 2000). These simulations show that cluster alignments are not crucial for discriminating between cosmological models, but they support the gravitational instability hypothesis of structure formation.

1.1. Optical Alignments

The projected shape of galaxy clusters on the sky are often elongated images (Carter & Metcalfe 1980) that can be approximately fit by ellipses. The major axes of these define projected position angles, measured counter-clockwise from north. Bingelli (1982) found that the major axes of galaxy clusters tend to point toward their nearest neighbor. Since then, there have been many optical studies of galaxy cluster alignments with their surroundings. Most of the literature finds alignment on some scale. For example, Flin (1987) and Rhee & Katgert (1987) found significant nearest neighbor alignment for separations, $d_n < 30 \text{ h}^{-1}\text{Mpc}$. West (1989) found that clusters that reside within the same supercluster are significantly aligned on scales of $30 \text{ h}^{-1}\text{Mpc}$, and possibly even out to $60 \text{ h}^{-1}\text{Mpc}$. Rhee, van Haarlem & Katgert (1992) also detected alignment for clusters within the same supercluster, but did not find significance for nearest neighbor alignment. Plionis (1994) found significant alignment for $d_n < 30 \text{ h}^{-1}\text{Mpc}$, with weaker signals for larger separations up to $60 \text{ h}^{-1}\text{Mpc}$. Strubles & Peebles (1985) did not detect a significant alignment signal (however, see Argyles *et al.* 1986).

1.2. X-ray Isophote Alignments

Individual galaxies may not be the best tracers of the shape of a cluster. Problems can arise from foreground/background contamination, as well as the contribution of a discrete noise term. However, it is believed that the X-ray emitting gas within a cluster traces its gravitational potential (Sarazin 1986). X-ray morphology is, then, probably the best observable for determining galaxy cluster shape and orientation. Likewise, since optical alignment has been measured and is well supported, X-ray isophotal alignment is crucial for understanding nearest neighbor cluster alignment.

Unfortunately, there have not been many X-ray alignment studies. Ulmer, McMillan, & Kowalski (1989–hereafter UMK) performed the first alignment study using *Einstein* data on 46 clusters and found no significant result. However, Chambers, Melott, and Miller (2000–hereafter CMM) recently re-examined the Ulmer et al. results using updated cluster positions and found a very strong signal. Rhee, van Haarlem & Katgert (RvHK 1992) used

the X-ray images of clusters in a study of supercluster member alignment. They examined clusters within the same supercluster and a significant signal for nearest neighbor alignment was not detected. However, West (1989) used convolved X-ray and optical data to find that clusters are aligned when they are members of the same supercluster. Further, West, Jones & Forman (1995) showed that the X-ray substructure within clusters tends to share the orientation with its local environment out to $10h^{-1}\text{Mpc}$. Of the above analyses, which all used *Einstein* X-ray imagery, only UMK and RvHK did nearest neighbor alignment studies, and neither found support for the hypothesis. However, CMM, West, and West, Jones and Forman find support for the hypothesis that the shapes of galaxy clusters are aligned with LSS environment (as traced by nearest neighbors). The amount and quality of X-ray cluster data since the UMK and RvHK analyses, along with the conflicting reports discussed above, prompts a new analysis of the nearest neighbor cluster alignment with X-ray isophotes.

In this paper we present results for three cluster samples with previously determined projected position angles. We also merge these to obtain a larger sample. Our goal is to use well-controlled samples to test whether the X-ray emitting gas within rich clusters is aligned with their nearest neighboring rich cluster. One of our adopted samples was previously tested for nearest neighbor alignment in cases where clusters were within the same supercluster; a significant signal was not detected (RvHK, see above). The other samples we adopt have not previously been tested (Mohr, Evrard, Fabricant & Geller 1996; Kolokotronis, Basilakos, Plionis & Georgantopoulos 2001). In an earlier work (CMM), we studied a subsample of cluster orientations previously examined by UMK. Although they did not find a signal for nonuniform orientations, we detected a significant signal for alignment by using the Wilcoxon rank-sum test. As the Wilcoxon rank-sum test (WRS hereafter) is more effective in testing for alignments, we will use it in the present study. We use $q_0 = 0$ and $h = 100H_0 \text{ km s}^{-1} \text{ Mpc}^{-1}$ throughout.

2. Data and Analysis

2.1. The Cluster Samples

We did a literature search for previously determined X-ray position angles. Rhee, van Haarlem & Katgert used 107 clusters of galaxies to study alignments within superclusters. Of these 107 clusters, 27 had X-ray position angles determined from *Einstein* imagery (Rhee & Latour 1991). They focused on the entire X-ray image, using the largest circular region centered on the peak of the X-ray emission. Although they found alignment with clusters when they were members of the same supercluster, they did not find significant alignment

for nearest neighbors. We therefore adopt these 27 RvHK clusters as one of our samples.

Mohr, Evrard, Fabricant & Geller (MEFG 1996) used a sample of 65 galaxy clusters observed by the *Einstein* IPC to constrain the range of cluster X-ray morphologies. They emphasized the core of the X-ray image. In this work, we are only concerned with Abell clusters. Since not all of these 65 are Abell clusters, we are left with 54 MEFG clusters.

Kolokotronis, Basilakos, Plionis & Georgantopoulos (KBPG 2001) found significant correlations between the optical and *ROSAT* X-ray shape parameters of 22 rich galaxy clusters. They conclude the dynamical state of clusters can be indicated by both parts of the spectrum. Their X-ray analysis focuses on the inner region of the images. We also use this sample of 22 KBPG clusters.

2.2. Nearest Neighbor Sample

We measure the nearest neighbor distances using rich ($R \geq 1$) clusters from the Abell(1958) and Abell, Corwin, and Olowin (1989) catalogs. To have a well controlled neighbor sample, we follow the strategy of CMM. As $R=0$ clusters are not part of Abell’s statistical sample, we only use $R \geq 1$ clusters in our study. Also, since more accurate redshifts are now available, we have updated the redshifts of all clusters. The redshifts and coordinates used are mainly from the MX Northern Abell Cluster Survey (MX; Slingend *et al.* 1998; Miller *et al.* 2001) and the ESO Nearby Abell Cluster Survey (Katgert *et al.* 1996). We use the richness values from the Abell catalog for the Abell/ACO overlap region ($-27^\circ \leq \delta \leq -17^\circ$). There are 336 rich ($R \geq 1$) clusters within the $|b| \geq 30^\circ$ and $0.012 \leq z \leq 0.10$ boundary of this survey. These clusters have on average 25 redshifts per cluster and 86% have at least two measured galaxy redshifts.

We search through the 336 rich clusters for possible nearest neighbors. We note that there are not many clusters with $d_n > 30h^{-1}\text{Mpc}$. A potential weakness of nearest neighbor studies is the neglect of the survey boundary location. Therefore, we note the distance and direction to the neighbor, and the distance to the boundary of the survey, all with respect to the subject cluster. Since a potential nearest neighbor may be hidden just outside the boundary, we disqualify any pair in which the distance to the boundary was less than the distance to the nearest neighbor.

We would like to briefly discuss the advantages of our controlled samples. By using $R \geq 1$ clusters, we are ensured that we have a statistically complete subsample. Miller *et al.* (1999) found that cluster mean redshifts based on only one galaxy redshift are often erroneous by $\sim 5 h^{-1}\text{Mpc}$, which can throw off the distance to the nearest neighbor and

perhaps more importantly, the identification and direction to the true nearest neighbor. Thus, updating the cluster redshifts makes sure that we are using the correct nearest neighbor (and nearest neighbor distance). And finally, excluding cases where the boundary distance is closer than the neighbor also helps to prevent the identification of an incorrect nearest neighbor.

2.3. Statistical Samples

After we apply these stringent criteria to our data, we are left with three statistical samples. Twenty seven of the RvHK clusters are rich and within the boundary of the survey. However, in four cases, the boundary was closer than the nearest neighbor. So we are left with 23 RvHK clusters. The sample of MEFG lost 25 clusters because of richness or not being within the survey volume. Of the 29 remaining, six pairs did not obey our nearest neighbor-boundary distance requirement: We are left with 23 MEFG clusters. Four of the original KBPG clusters did not obey the richness-boundary criteria. And five of the 18 remaining clusters had the boundary distance closer than the neighbor. That is, we have 13 KBPG clusters after our cuts. In summary, our statistical samples for RvHK, MEFG and KBPG contain 23/27, 23/54 and 13/22 clusters, respectively.

We also merged these three samples. We start with 59 objects from our three controlled statistical samples. Some clusters appear in more than one statistical samples, so there are actually 48 Abell clusters to consider. That is, there are 11 Abell clusters with two independently measured orientations. Nine of these clusters are common to the MEFG and RvHK samples; the other two Abell clusters are in both MEFG and KBPG. We have kept nine out of these 11 clusters, discarding two (common to MEFG and RvHK) because of inconsistent orientations. We tested the independently determined position angles and found they are highly correlated. We alternately choose the angles to use by chronology in Abell number, keeping four RvHK, three MEFG and the two KBPG. This makes a total of 46 total clusters in our merged sample.

2.4. Analysis

Position angles, measured counter-clockwise from north, were previously provided for our statistical samples by the named authors. The projected angular difference between this angle and the direction to the nearest neighbor defines the pointing angle, ϕ_p . We are concerned with the orientation of the subject cluster with respect to its nearest neighbor,

so we neglect signs and thus the pointing angle ranges as $0^\circ \leq |\phi_p| \leq 90^\circ$.

We define alignment as the tendency for the pointing angles, $|\phi_p|$, to be systematically smaller than they would be if distributed isotropically over this interval. The Wilcoxon rank-sum test (WRS; Lehmann 1975) tests for this. The null hypothesis of WRS is that the sample is not systematically smaller or larger than the (uniform) parent population (refer to CMM for more details).

We test our statistical samples and merged sample for nearest neighbor alignment at various maximum nearest neighbor distances, D_{max} . All four samples show the same general trend. When $D_{max} \geq 30 \text{ h}^{-1}\text{Mpc}$ signals for alignment are low. However, restricting $D_{max} \leq 20 \text{ h}^{-1}\text{Mpc}$, we generally find significant signals for alignment; in some cases the significance declines for smaller D_{max} due to many fewer cluster pairs. In fact, all samples except KBPG have maximum significance for alignment at $D_{max} \leq 10 \text{ h}^{-1}\text{Mpc}$. It should be noted, however, that KBFG suffers from sparseness more than the other samples, and its utility is reflected better in the merged sample. The increased number of objects in the merged sample is a tremendous improvement over the sparser statistical samples. For example, at $D_{max} \leq 20 \text{ h}^{-1}\text{Mpc}$, with 33 clusters, the merged sample has a large 3.57σ signal for alignment; and when $D_{max} \leq 10 \text{ h}^{-1}\text{Mpc}$, the significance reaches a maximum of 4.95σ for 19 clusters.

Table 1 shows the results of WRS our three statistical samples and the merged sample. We have included D_{max} , significance and the number of clusters, N_{cl} , within D_{max} . Note the increase in significance for smaller D_{max} .

3. Conclusion and Discussion

We tested three samples of previously determined X-ray position angles, 46 clusters total, for nearest neighbor alignment. We found, using the Wilcoxon rank-sum (WRS) test, that the X-ray isophotes in our samples are aligned with their nearest neighboring rich Abell cluster, consistent with the gravitational instability hypothesis (Shandarin & Klypin 1984). We noted a trend where alignment significantly increases as the maximum neighbor distance is decreased. In fact, we noticed a transition zone, before which isophote alignment becomes significant. The merged sample, which represents the statistical samples well, illustrates this trend. For example, with no restrictions on d_n , it has a 1.06σ signal. However, at $d_n \leq 20 \text{ h}^{-1}\text{Mpc}$, the merged sample has 3.57σ significance for nearest neighbor alignment; and 4.08σ for $d_n \leq 15 \text{ h}^{-1}\text{Mpc}$. The confidence reaches a maximum of 4.95σ when $d_n \leq 10 \text{ h}^{-1}\text{Mpc}$. Therefore, our data shows that the orientation of the X-ray emitting gas within

rich clusters is correlated with nearest rich neighbor positions when $d_n \leq 20 \text{ h}^{-1}\text{Mpc}$; this distance roughly marks a transition zone from orientations being random to aligned. This transition distance is the same found by Novikov, *et al.* (1999) for alignment between cluster winds and the neighboring cluster population. It likely represents the wavelength undergoing collapse at this time in cosmic history, the so-called “pancaking scale” (Melott & Shandarin 1993; Shandarin *et al.* 1995).

Moreover, we found high confidence for nearest neighbor alignment in the RvHK sample, who previously had not detected a significant signal (though they concentrated on clusters that were members of the same supercluster). We speculate that updated redshifts may have changed supercluster member positions, and consequently nearest neighbors. Our RvHK signal is 2.72σ for $d_n \leq 20 \text{ h}^{-1}\text{Mpc}$, and reaches 3.77σ when $d_n \leq 10 \text{ h}^{-1}\text{Mpc}$. In a previous work (CMM 2000) we also showed the X-ray data of Ulmer, McMillan and Kowalski (UMK 1989) exhibits alignment, contrary to their conclusions. Using a consistent data analysis and a clear statistical methodology, we have removed two crucial discrepancies from X-ray alignment studies; now, all samples tested (to our knowledge) have been shown to exhibit significant X-ray alignment on similar scales.

4. Acknowledgments

ALM and SWC are grateful for financial support under NSF grant AST-0070702 and computing resources from the National Center for Supercomputing Applications.

REFERENCES

- Abell, G. O., 1958, ApJS, 3, 211
Abell, G. O., Corwin Jr., H.G., Olowin, H.G., 1989, ApJS, 70, 1
Argyres, P. C., Groth, E. J., Peebles, P. J. E., Struble, M. F., 1986, ApJ, 91, 471
Binggelli, B. 1982, A&A, 107, 338
Carter, D., and Metcalfe, N. 1979, MNRAS, 191, 325
Chambers, S.W., Melott, A.L., Miller, C.J., 2000, ApJ, 544, 104
Flin P. 1987, MNRAS, 228, 941
Kolokotronis, V., Basilakos, S., Plionis, M., Georgeantopoulos, I., 2001, MNRAS, 320, 49
Katgert, P., et al. 1996, A&A, 310, 8

- Lehmann, E.L. 1975 *Nonparametrics: Statistical Methods Based on Ranks* (Prentice Hall: New Jersey)
- Melott, A.L., & Shandarin, S.F., 1993, *ApJ*, 410, 496
- Miller, C., & Batuski, D. 2000, submitted to *ApJ*(astro-ph/0002295)
- Miller, C.J., Batuski, D.J., Slingland, K.A., and Hill, J.M. 1999 *ApJ* 523, 492
- Miller, C.J., Krughoff, K.S., Batuski, D.J., Slingland, K.A., & Hill, J.M. 2000, submitted to *AJ*
- Mohr, J.J, Evrard, A.E., Fabricant, D.G & Geller, M.J., 1995, *ApJ*, 447, 8
- Novikov, D.I., Melott, A.L., Wilhite, B.B., Kaufman, M., Burns, J.O., Miller, C.J, and Batuski, D.J., 1999 *MNRAS*, 304, L5
- Onuora, L.I. and Thomas, P.A., 2000 *MNRAS*, 1995, *ApJ*, 447, 8 in press (astro-ph/0003402)
- Plionis, M., 1994, *ApJ* 95, 401
- Rhee, G.F.R.N., Katgert P., 1987, *A&A*, 183, 217
- Rhee, G.F.R.N. & Latour, H.J., *A&A*, 243, 38
- Rhee G.F.R.N., van Haarlem M., Katgert P., 1992, *AJ*, 103, 1721
- Sarazin, C.L., 1986, *Rev. Mod. Phys.*, 58, 1
- Shandarin, S.F., and Klypin, A.A. 1984, *Sov Astron.* 28, 491
- Shandarin, S.F., Melott, A.L., McDavitt, K., Pauls, J.L., & Turner, J., 1995, *Phys.Rev.L*, 75, 7
- Slingland, K., Batuski, D., Miller, C., Haase, S., Michaud, K., & Hill, J. 1998, *ApJS*, 115, 1
- Splinter R.J., Melott A.L., Linn, A.M., Buck C., Tinker J., 1997, *ApJ* 479, 632
- Struble M.F., Peebles P.J.E., 1985, *AJ*, 90, 592
- Ulmer M.P., McMillan S.L.W., Kowalski M.P., 1989, *ApJ*, 338, 711
- West M.J., 1989, *ApJ*, 347, 610
- West M.J., Jones C., Forman W., 1995, *ApJ*, 451, L5

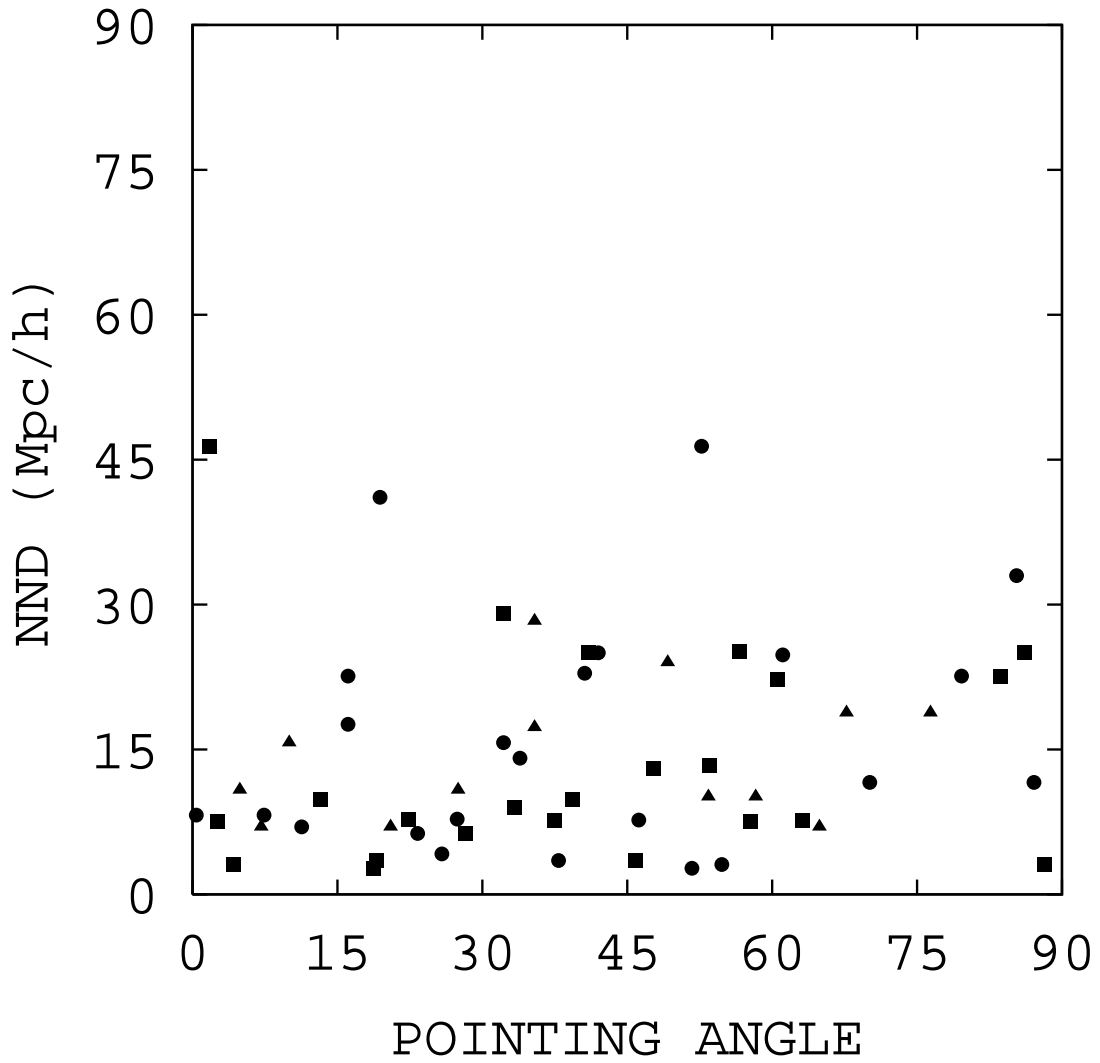


Fig. 1.— The distribution of pointing angle against nearest neighbor distance is shown for our 59 samples. Squares represent RvHK data; Circles, MFEG; Triangles, KBFG.

Table 1. WRS Results for the Statistical Samples

D_{max} ($h^{-1}\text{Mpc}$)	RvHK		MEFG		KBPG		Merged	
	Sig.	N_{cl}	Sig.	N_{cl}	Sig.	N_{cl}	Sig.	N_{cl}
10	3.77σ	14	3.10σ	10	1.85σ	3	4.95σ	19
15	2.72σ	16	1.81σ	13	3.25σ	7	4.08σ	28
20	2.72σ	16	2.23σ	15	0.83σ	11	3.57σ	33
30	0.60σ	22	1.49σ	20	0.44σ	13	1.61σ	44
None	0.44σ	23	0.56σ	23	0.43σ	13	1.06σ	46